13th World Conference on Earthquake Engineering
Vancouver, B.C., Canada
August 1-6, 2004
Paper No. 3387

NUMERICAL MODELING OF DYNAMIC CENTRIFUGE TESTS

Peter M. BYRNE[1], Sung-Sik PARK[2], Michael BEATY[3], Michael SHARP[4], Lenart GONZALEZ[5] and Tarek ABDOUN[6]

SUMMARY

The prediction of liquefaction and resulting displacements is a major concern for earth structures located in regions of moderate to high seismicity. Conventional procedures used to assess liquefaction commonly predict the triggering of liquefaction to depths of 50 m or more. Remediation to prevent or curtail liquefaction at these depths can be very expensive. Field experience during past earthquakes indicates that liquefaction has mainly occurred at depths less than about 15 m, and some recent dynamic centrifuge model testing initially appeared to confirm a depth or confining stress limitation on the occurrence of liquefaction. Such a limitation could greatly reduce remediation costs. In this paper an effective stress numerical modeling procedure is used to assess these centrifuge tests. The results indicate that a lack of complete saturation as well as densification at depth arising from the application of the high acceleration field are largely responsible for the apparent limitation on liquefaction at depth observed in some centrifuge tests.

INTRODUCTION

The prediction of liquefaction and resulting displacements is a major concern for earth structures located in regions of moderate to high seismicity. This is particularly so for earth dams where large displacements could lead to overtopping and sudden release of the reservoir with life safety concerns.

The standard procedure used to assess liquefaction commonly predicts the triggering of liquefaction to depths of 50 m or more. Remediation to prevent or curtail liquefaction at these depths can be very expensive. Field experience during past earthquakes (Youd [1]) indicates that liquefaction has mainly occurred at depths less than 15 m, and some recent dynamic centrifuge model testing (Steedman [2]) suggests a depth or confining stress limitation on the occurrence of liquefaction. Such a limitation on

[1] Professor Emeritus, Dept. of Civil Engineering, Univ. of British Columbia, Vancouver, BC, Canada
[2] Graduate Student, Dept. of Civil Engineering, Univ. of British Columbia, Vancouver, BC, Canada
[3] Senior Engineer, Calif. Dept. of Water Resources, Sacramento, CA, USA
[4] Director, Centrifuge Research Center, Engineer Research and Development Center, Vicksburg, MS, USA
[5] Research Assistant, Dept. of Civil Engineering, Rensselaer Polytechnic Institute, Troy, NY 12180, USA
[6] Research Assistant Professor, Dept. of Civil Engineering, Rensselaer Polytechnic Institute, Troy, NY 12180, USA

excess pore pressure development could greatly reduce remediation costs, but confirmation requires reliable data and an improved understanding of the liquefaction process through analysis.

Liquefaction can be assessed from total or effective stress analyses. Effective stress analyses have been available for more than 25 years and are more fundamental. Triggering of liquefaction as well as post-liquefaction stability and resulting displacements can be considered in a single time domain analysis. Such analyses are generally based on capturing the element behaviour from laboratory tests and then considering the soil structure to comprise a collection of such elements with both generation and dissipation of pore water pressure occurring as shaking proceeds. In this way the weaker and/or more heavily loaded elements are predicted to liquefy first, and the resulting displacements increase with time in a phenomenon referred to as lateral spreading. If sufficient elements liquefy and their residual strength is insufficient for static stability, a flow slide will result. Effective stress analyses have the capability of predicting observed liquefaction response.

The validation of effective stress modeling is very important, but it is difficult to achieve from field case histories because the soil conditions and input motion are seldom known with sufficient accuracy. The best documented case histories are the Upper and Lower San Fernando dams and their response to the 1971 San Fernando earthquake, but even for these cases there is considerable uncertainty about conditions and loading.

Model tests can be conducted in the laboratory under controlled conditions and their response observed. However, because soil behavior is highly stress dependent, small models under a one “g” acceleration field are not representative of field conditions. On the other hand, centrifuge tests that utilize a high acceleration field preserve the stress-strain response of the prototype soil and can give a more realistic representation of field behaviour. Such models, when subjected to a controlled base motion, can provide a database for the validation of numerical approaches.

Although centrifuge testing provides a seemingly ideal tool for validating numerical models, their application is not always straightforward. A major validation initiative (Arulanandan [3]) using centrifuge tests was carried out in the 1990’s and was termed a mitigated disaster by Prof. Ronald Scott in his oral presentation. Some of the reasons for this assessment were due to aspects of the centrifuge tests including the boundary conditions in the centrifuge box, the use of water as a pore fluid and the resulting high rate of drainage, and the lack of verification of saturation. The validation process also showed the necessity of models to rationally consider the generation and dissipation of excess pore pressure during shaking. At that time, a very limited number of numerical models were successful in accomplishing this task.

In this paper a numerical procedure is used in which both generation and dissipation of pore fluid pressure is considered. The procedure is applied to predict the results of centrifuge tests that investigate liquefaction at large depths. The characteristic liquefaction behaviour of Nevada sand used in the models was obtained from undrained cyclic simple shear tests and is the basis for the numerical predictions of the centrifuge tests. Several factors had to be considered to accurately predict the centrifuge results including the change in density caused by the confining stresses induced in the centrifuge, and the effects of degree of saturation.

A comparison of predicted and measured centrifuge model response is presented in this paper. Prior to the prediction, a brief description of the numerical model is presented. In addition, the effects of saturation and stress-densification on liquefaction response are discussed.

EFFECTIVE STRESS NUMERICAL MODELLING OF LIQUEFACTION

Fully coupled effective stress approaches which consider shear induced pore pressures at each time step rather than at each cycle or half cycle have been developed by many researchers including Dafalias [4], Prevost [5], Zienkiewicz [6], Byrne [7], Beaty [8], Elgamal [9], and Kramer [10]. The numerical procedure used in this paper is a fully coupled approach called UBCSAND (Puebla [11], Beaty [8], Byrne [12]). It is based on plasticity theory and the characteristic sand behaviour observed in laboratory tests under monotonic and cyclic loading conditions. It is presented briefly below.

Elastic response

The elastic component of response is assumed to be isotropic and specified by a shear modulus, G^e, and a bulk modulus, B^e, as follows:

[1] $$G^e = K_G^e \cdot P_a \cdot \left(\frac{\sigma'}{P_a}\right)^{ne}$$

$$B^e = \alpha \cdot G^e$$

where K_G^e = a shear modulus number that depends on the density of the sand and varies from about 500 for loose sand to 2000 for dense sand; P_a is atmospheric pressure in the chosen units; σ' is the mean stress in the plane of loading; ne is an elastic exponent that varies between 0.4 and 0.6, or approximately 0.5; and α depends on the elastic Poisson's ratio which is in the range 0.0 ~ 0.2 (Hardin [13]) with the result that α varies between 2/3 and 4/3 or is approximately unity.

Plastic response

Plastic strains are controlled by the yield loci, which are assumed to be radial lines starting at the origin of stress space as shown in Fig. 1. For first time shear loading, the yield locus is controlled by the current stress state, point A in Fig. 1. As the shear stress increases, the stress ratio $\eta (= \tau / \sigma')$ increases and causes the stress point to move to point B. τ and σ' are the shear and normal effective stresses on the plane of maximum shear stress. The yield locus is dragged to the new location passing through point B and the origin. This results in plastic strains, both shear and volumetric. The plastic shear strain increment, $d\gamma^p$, is related to the change in shear stress ratio, $d\eta$, as shown in Fig. 2 and can be expressed as

[2] $$d\gamma^p = \frac{1}{G^p / \sigma'} \cdot d\eta$$

where G^p is the plastic shear modulus and, assuming a hyperbolic relationship between η and γ^p, is given by:

[3] $$G^p = G_i^p \cdot \left(1 - \frac{\eta}{\eta_f} \cdot R_f\right)^2$$

where G_i^p is the plastic modulus at low stress ratio level $(\eta = 0)$, η_f is the stress ratio at failure and equals $sin\phi_f$, where ϕ_f is the peak friction angle, and R_f is the failure ratio used to truncate the best fit hyperbolic relationship and prevent the overprediction of strength at failure. R_f generally varies between 0.7 and 0.98 and decreases with increasing relative density. It has been useful to relate G_i^p to G^e and relative density D_r, through the approximate relationship $G_i^p \approx 3.7 \cdot (D_r)^4 \cdot G^e + P_a$.

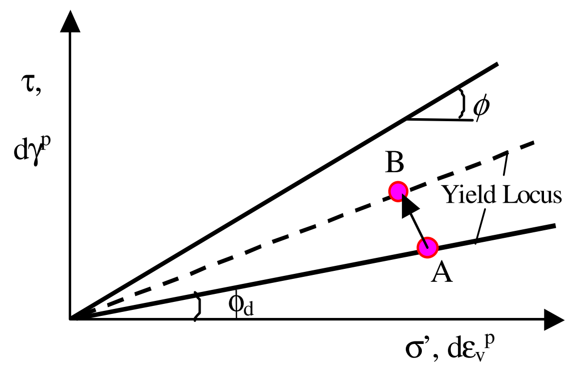

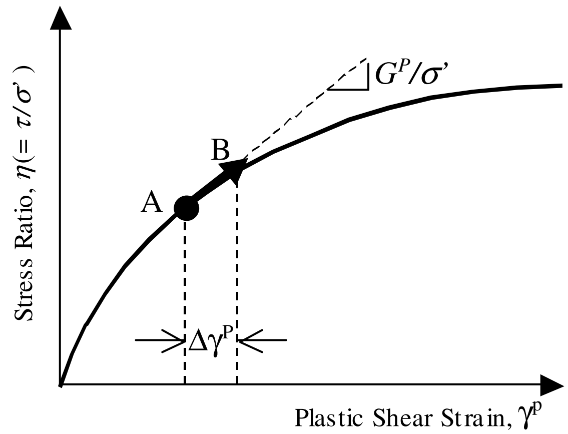

Fig. 1 Yield locus **Fig. 2 Plastic strain increment and plastic modulus**

The associated increment of plastic volumetric strain, $d\varepsilon_v^p$, is related to the increment of plastic shear strain, $d\gamma^p$, through the flow rule as follows:

[4] $$d\varepsilon_v^p = (sin\phi_{cv} - \frac{\tau}{\sigma'}) \cdot d\gamma^p$$

where ϕ_{cv} is the constant volume friction angle or phase transformation angle.

The yield loci and direction of the plastic strains resulting from the flow rule are shown in Fig. 3. It may be seen that at low stress ratios, significant shear induced plastic compaction is occurring, while no compaction is predicted at stress ratios corresponding to ϕ_{cv}. For stress ratios greater than ϕ_{cv}, shear induced plastic expansion or dilation is predicted. This simple flow rule is in close agreement with the characteristic behaviour of sand observed in laboratory element testing. Upon unloading (reducing stress ratio), the sand is assumed to behave elastically. Upon reload, the sand is assumed to behave plastically but with a plastic modulus that is several times stiffer than for first time loading until the prior maximum value is reached at which point it reverts to first time loading.

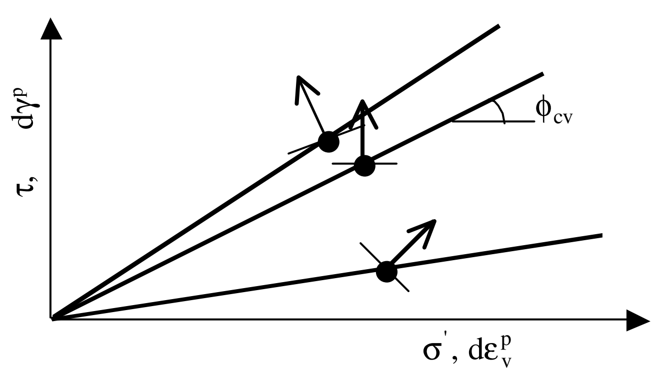

Fig. 3 Direction of plastic strains (flow rule)

The response of sand is controlled by the skeleton behaviour. A fluid (air water mix) in the pores of the sand acts as a volumetric constraint on the skeleton if drainage is curtailed. It is this constraint that causes the pore pressure rise that can lead to liquefaction. Provided the skeleton or drained behaviour is appropriately modeled under monotonic and cyclic loading conditions, and the stiffness of the pore fluid and drainage are accounted for, the liquefaction response can be predicted for any partially saturated and partially drained conditions. This is the approach taken here and the concepts discussed above are incorporated in UBCSAND.

This model was used with the computer code FLAC (Fast Lagrangian Analysis of Continua) Version 4.0 (Itasca [14]). This program models the soil mass as a collection of grid zones or elements and solves the coupled stress flow problem using an explicit time stepping approach. The program has a number of built-in stress-strain models including an elastic plastic Mohr-Coulomb model, and UBCSAND is a variation of this model in which friction and dilation angles are varied to incorporate the yield loci and flow rule described above. Pore fluid stiffness and Darcy hydraulic flow are basic to the FLAC program so that only the skeleton stress-strain relation is needed to simulate liquefaction. Drained, undrained, or coupled stress flow conditions are specified by the user.

CENTRIFUGE TESTS OVERVIEW

Centrifuge tests to evaluate liquefaction response at high confining stress have been carried out at the US Army Corp of Engineers, Engineer Research and Development Center (ERDC), Vicksburg. These tests were basically comprised of a dense sand layer with $D_r \approx 80$ % overlying a loose sand layer with $D_r \approx 50$ %. High confining stresses were achieved by application of a surface layer of lead.

The soil used for these tests was Nevada sand. Preliminary centrifuge results were presented by Steedman [2] and indicated that there is a cut-off confining pressure above which liquefaction will not occur. The data suggests this pressure is about 300 kPa, and the authors contend that field evidence supports this finding. If this is the case then huge savings in retrofit costs for many existing dams and bridges is possible, since present analyses procedures indicate that treatment to curtail or prevent liquefaction is often necessary to depths where pressures are well in excess of 300 kPa.

To verify such a cut-off, additional centrifuge tests were carried out at RPI (Gonzalez [15]). These tests indicated no cut-off confining stress for stresses up to 380 kPa, but did show trends in the development of pore pressure and liquefaction that were not consistent with state of practice or with state-of-art liquefaction analysis.

There are a number of possible reasons for the differences between the two sets of centrifuge data and current analysis procedures including: i) characteristics of the centrifuge model containment box; ii) saturation of the model and pore fluid stiffness; and iii) stress densification effects. These possibilities are briefly discussed below, followed by a more detailed discussion of stress densification and pore fluid stiffness.

Characteristics of the Containment Box

In both ERDC and RPI tests a laminar box comprised of rings allowing lateral shear movements (lateral strain in the long direction of the box, parallel to shaking) was used. The ERDC box had a stiff sealant between rings, while in the RPI box, the rings are separated by linear roller bearings (free to slide laterally). Therefore upon liquefaction, the ERDC box could offer significant lateral resistance that could influence the dynamic response of the model and the measured accelerations.

Model Saturation

The RPI models were saturated using a process that involved replacement of air with carbon dioxide gas and then displacement and dissolving of the gas by introduction of high viscosity water under vacuum. In the ERDC tests, the viscous fluid was introduced at the base of the sample without prior removal of air by carbon dioxide or application of vacuum. In neither case was the degree of saturation or stiffness of the pore fluid evaluated by measurement of the compression wave or other means.

Stress Densification

The density of the sand in the model will change with stress. The authors believe that at high confining stress such changes could be quite significant and impact the numerical modeling of the soil response. Stress densification effects in sand have been discussed by Park [16].

Purpose of Numerical Analyses

The purpose of the effective stress analysis carried out here is to a obtain a measure of understanding of the importance of various aspects of the testing including the degree of saturation of the pore fluid and stress densification effects. Prior to examining the centrifuge data and the results of the analyses, the effect of pore fluid stiffness will be addressed.

EFFECT OF PORE FLUID STIFFNESS ON GENERATED PORE PRESSURES

The pore pressures of concern for liquefaction are those generated by plastic volumetric strain. Pore pressures may also be generated by transient changes in total stress, but these lead to small changes in effective stress unless the soil is partially saturated. An applied load increment will induce a total volumetric strain increment, $d\varepsilon_v$, that is the sum of the elastic and plastic increments, $d\varepsilon_v^e$ and $d\varepsilon_v^p$. For undrained conditions the resulting change in pore pressure, *du,* is

[5] $$du = \frac{B_f}{n} \cdot d\varepsilon_v$$

where B_f is the bulk stiffness of the pore fluid (air water mix) and *n* is the porosity. The corresponding change in effective mean stress, $d\sigma'$, to an increment of volumetric strain is

[6] $$d\sigma' = B^e \cdot d\varepsilon_v^e \, .$$

The increment of total mean stress, $d\sigma$, is equal to the increment of effective mean stress and pore pressure. If, for simplicity we assume $d\sigma = 0$, then $du = -d\sigma'$, and from equations 5 and 6:

[7] $$du = \frac{B^e}{1 + \dfrac{B^e}{B_f / n}} \cdot d\varepsilon_v^p \quad = B_{skem} \cdot B^e \cdot d\varepsilon_v^p$$

where B_{skem} is the Skempton value commonly used to assess the saturation of samples in the laboratory. It is clear that the ratio of the skeleton stiffness to pore fluid stiffness, B^e / B_f, is a major factor in pore pressure response.

From Boyle's law, and assuming the same pressure in both water and air, B_f is found to be a function of *p*, the current absolute pressure of the fluid, and S_{ro}, the saturation at zero gauge pressure (*p* = 100 kPa), as given by

[8] $$B_f \cong \frac{p^2}{(1 - S_{ro}) \cdot P_a} \quad < \text{ 2e6 kPa}$$

S_{ro} is the initial saturation in a centrifuge model prior to spin up. If the pores are completely filled with water then B_f = 2e6 kPa, the bulk stiffness of water. If B^e = 6e4 kPa and n = 1/3, then B_{skem} = 0.99 and $du = 0.99 \cdot B^e \cdot d\varepsilon_v^p$. But if the degree of saturation were reduced to S_{ro} = 0.98, then B_f drops to 5000 kPa at p = 100 kPa, with B_{skem} = 0.2 and $du = 0.2 \cdot B^e \cdot d\varepsilon_v^p$.

Poor saturation at low pore pressure will lead to a reduced pore pressure response to load. This is particularly so if the skeleton stiffness is high. This may occur in a centrifuge model near the water table when it is at depth or when a surface load is applied. For a water table at the surface and no surface load, B_{skem} may still be high as the skeleton stiffness will be low.

If the water pressure p in the soil increases, as it would during spin up, then water will flow into the voids, compress the air, and increase B_f. This increase in fluid stiffness with pressure is included in equation 8 and the subsequent numerical simulations. Initial degrees of saturation in excess of 99.9 % are required to obtain B_f > 5e5 kPa for pore pressures less than 100 kPa gauge. Such values of B_f will generally produce a liquefaction response similar to a fully saturated condition. Initial saturation is seen to be very important and can have a very large effect on pore pressure rise and liquefaction response.

PROPERTIES OF NEVADA SAND

The properties for Nevada sand used in the centrifuge tests and the modeling are as follows:

Hydraulic Conductivity, k

The hydraulic conductivity, *k*, used in the analyses is based on constant head permeability tests carried out for the VELACS program (Arulmoli [17]). The results are shown in Fig. 4 where *k* varies between 6.6×10^{-5} m/sec at low relative density to 2.3×10^{-5} m/sec at high relative density. The values shown are for water as a pore fluid under a 1 *g* field. For centrifuge tests in an acceleration field "*N*" times greater than gravity, the effective *k* will be *N* times greater. If the viscosity of the fluid is *M* times greater than water as it may be for the centrifuge tests, then k would reduce by a factor *M*. Thus:

[9] $$k^* = k\frac{N}{M}$$

where k^* is the effective hydraulic conductivity in the centrifuge and *k* is the hydraulic conductivity of the soil in a 1 *g* environment using water as a pore fluid.

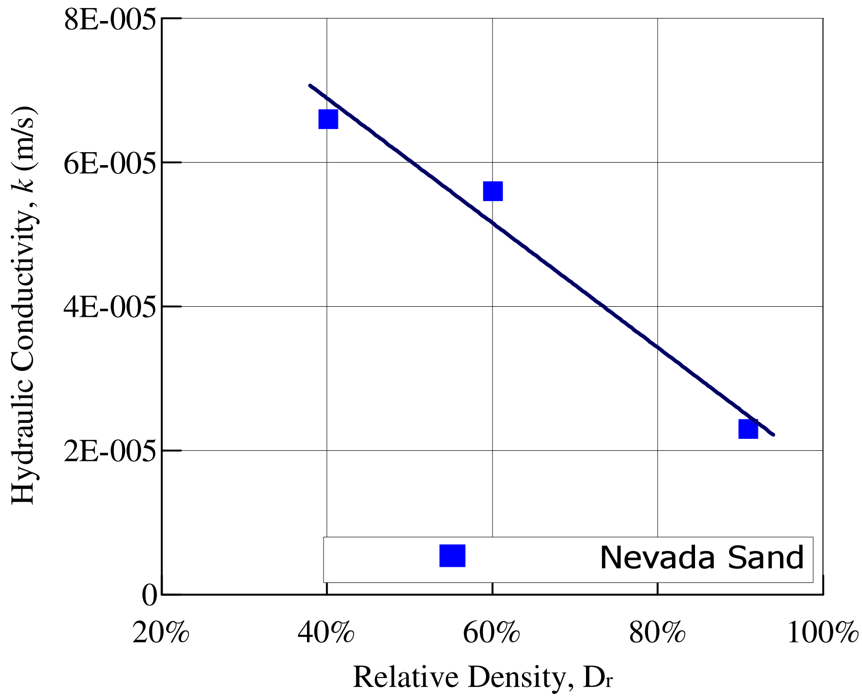

Fig. 4 Hydraulic conductivity of Nevada sand (Arulmoli [17])

Liquefaction Resistance

The liquefaction response of Nevada sand was based on cyclic simple shear tests carried out for the VELACS project (Arulmoli [17]) as well as tests carried out at the University of California at Berkeley (Kammerer [18]). The results of these tests are shown in Fig. 5 in terms of cyclic stress ratio vs. number of cycles to liquefaction for a range of relative densities. The predicted liquefaction response of the sand from the numerical model for a fully saturated state is shown by the lines on Fig. 5, which capture the data quite well. For both the laboratory tests and the numerical model, liquefaction was assumed to occur when the cyclic strain amplitude reached 3.75 %.

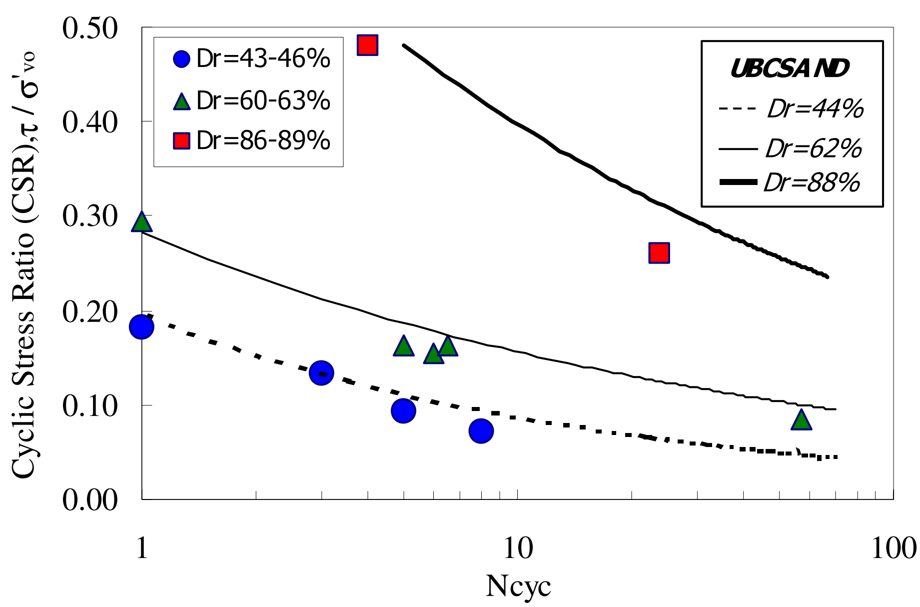

Fig. 5 Cyclic resistance of Nevada sand (Arulmoli [17]; Kammerer [18])

CENTRIFUGE TESTS RESULTS AND ANALYSIS

Two centrifuge model tests conducted at the RPI centrifuge facility (Models 1 and 2) as well as one from ERDC (Model 5a) were examined in detail. The models are comprised of Nevada sand and simulate level ground conditions subjected to a harmonic base input motion. The frequency of the input motion was selected to reduce the potential for amplification in the model.

Centrifuge Model 1

Model 1 is comprised of a uniform sand layer with a placed relative density D_r = 55 %. It was subjected to an acceleration field of 120 g and the fluid viscosity was 60 times that of water. The fluid table is at the surface of the model. No surcharge was applied at the surface, and the maximum initial effective stress at the base was 380 kPa.

Centrifuge Model 2

Model 2 is comprised of a dense layer D_r = 75 % overlying a looser layer, D_r = 55 %. It was subjected to an acceleration field of 80 *g* and had a surface load of 140 kPa. This condition also gave an effective stress at the base of 380 kPa.

Centrifuge Model 5a

Model 5a is comprised of a dense layer D_r = 72 % overlying a looser layer, D_r = 51 %. It was subjected to an acceleration field of 50 *g* and had a surface load of 580 kPa. This condition gave an effective stress at the base of 836 kPa.

Numerical Models

The centrifuge models were analyzed with a single column of elements. This one-dimensional representation is equivalent to assuming the stresses and strains in the centrifuge model are uniform across any horizontal plane. Boundary constraints were placed on the model so that the top of each soil element remained horizontal during loading and the width of the model remained virtually constant. This allowed each element to compress or expand in a vertical direction and to experience shearing deformations due to horizontal shear stresses. Secondary response modes, such as rocking, were not represented.

Initial saturation was not measured in any of the 3 models. An assumption of 100 % saturation led to predictions of excess pore pressure rise that were significantly faster than observed. Assumed saturation values of about 98.5 % before spinup were found to give best agreement with the measurements for the 2 RPI models (Models 1 and 2).

Results for RPI Model 1

A cross-section of Model 1 showing the locations of the pore pressure transducers and accelerations together with the FLAC simulation model is shown in Fig. 6. The input motion comprised 50 cycles of 0.2 g at 1.5 Hz prototype scale. The actual input motion amplitude varied somewhat with time as shown in Fig. 7 and this was used in the FLAC simulation. The effect of stress densification on relative density D_r was based on test results from Nevada sand (Park [16]) and is shown in Fig. 8. The relationship indicates that D_r has increased from 55 % to about 63 % near the base of the layer due to increased stress upon spin-up.

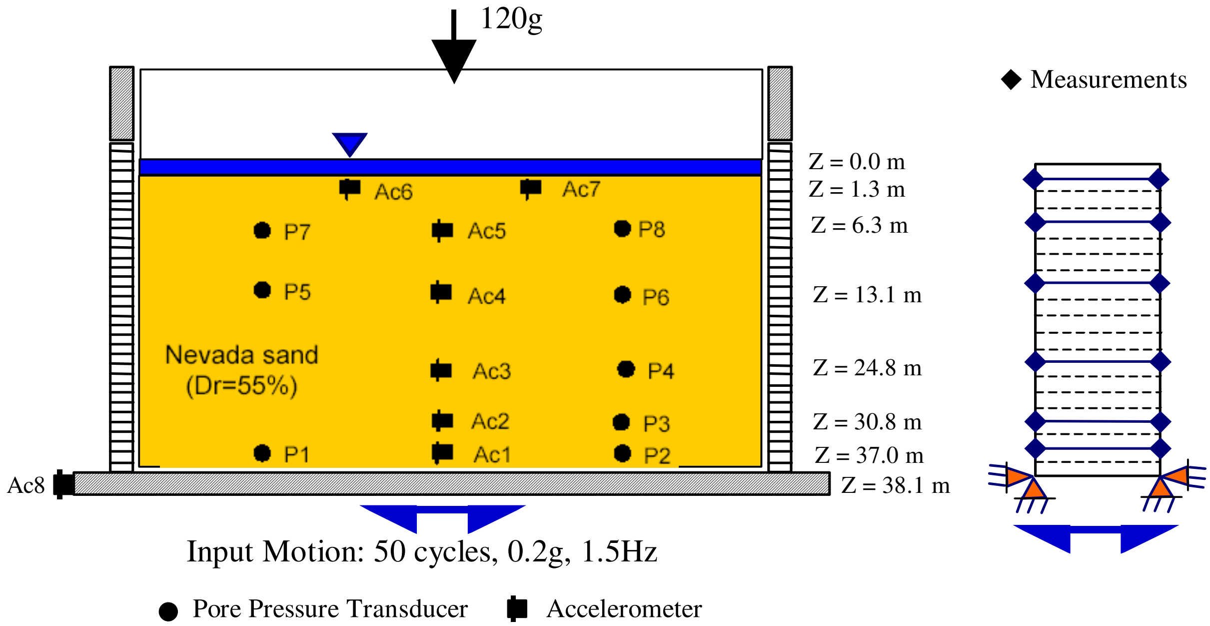

Fig. 6 Centrifuge Model 1 setups and FLAC Model 1 measurements

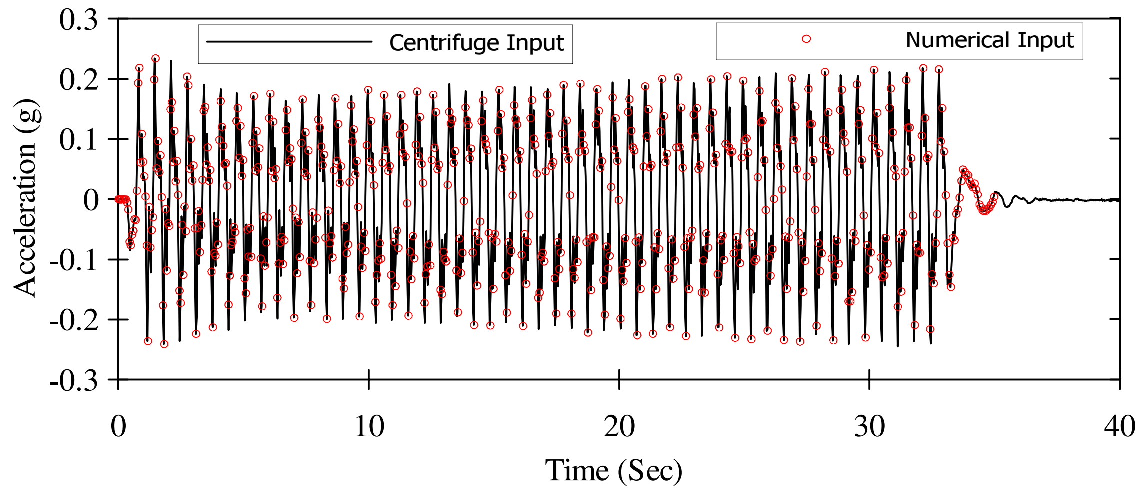

Fig. 7 Based input motions of Model 1

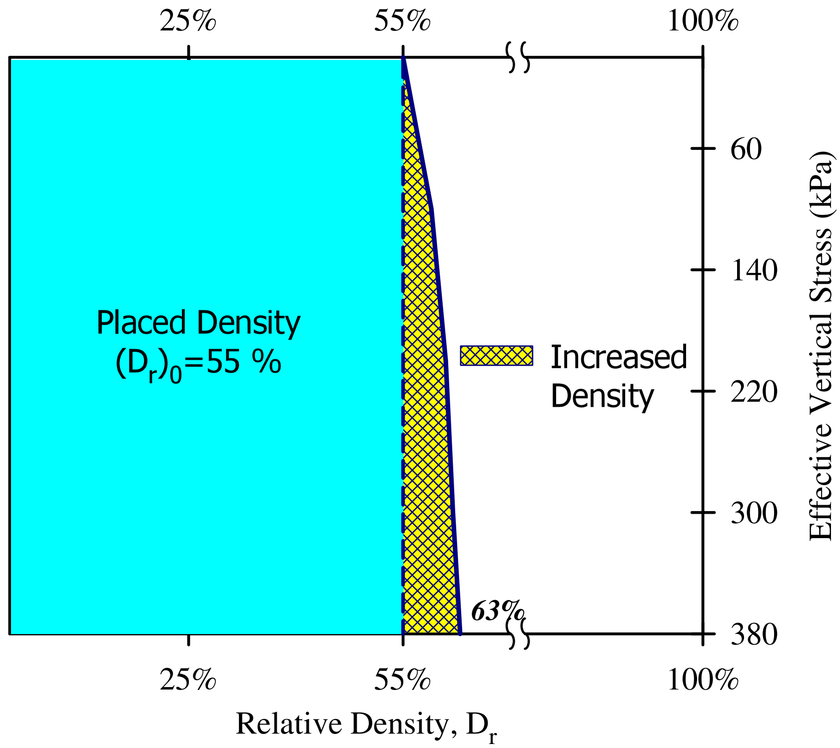

Fig. 8 Placed density and increased density of Model 1

The measured and predicted acceleration and excess porewater pressure time histories at prototype depths of 1.3, 6.3, 13.1, 24.8, 30.8 and 37.0 m are shown in Figs. 9a and 9b. It may be seen that, apart from the depth of 30.8 m, the patterns of predicted accelerations are in good agreement with the measurements. It is apparent from the large reduction in acceleration amplitude with time that liquefaction has occurred first at or near the surface and worked its way downward. It may also be seen from Fig. 9b that the predicted excess pore pressures are in good agreement with the measured values. At a depth of 13.1 m the excess porewater pressure has reached the initial vertical effective stress corresponding to 100 % pore pressures rise at a time of 6 sec indicating liquefaction. This time is in good agreement with the change in acceleration pattern.

The time to reach 100 % pore pressure rise increases with depth indicating that liquefaction occurs first near the surface and works its way downward. This is a somewhat surprising result as the accelerations in the initial time phase are about the same at all depths, perhaps somewhat higher at depth. This leads to a constant applied stress ratio, and if D_r were constant, standard practice would suggest that liquefaction should first be triggered at the base due to the K_σ effect. When the numerical simulation was carried out assuming constant D_r with depth, the liquefaction did occur first at the base and then work its way upward. Only when increased density at depth in accordance with stress densification was considered did the analysis predict the observed pore pressure pattern.

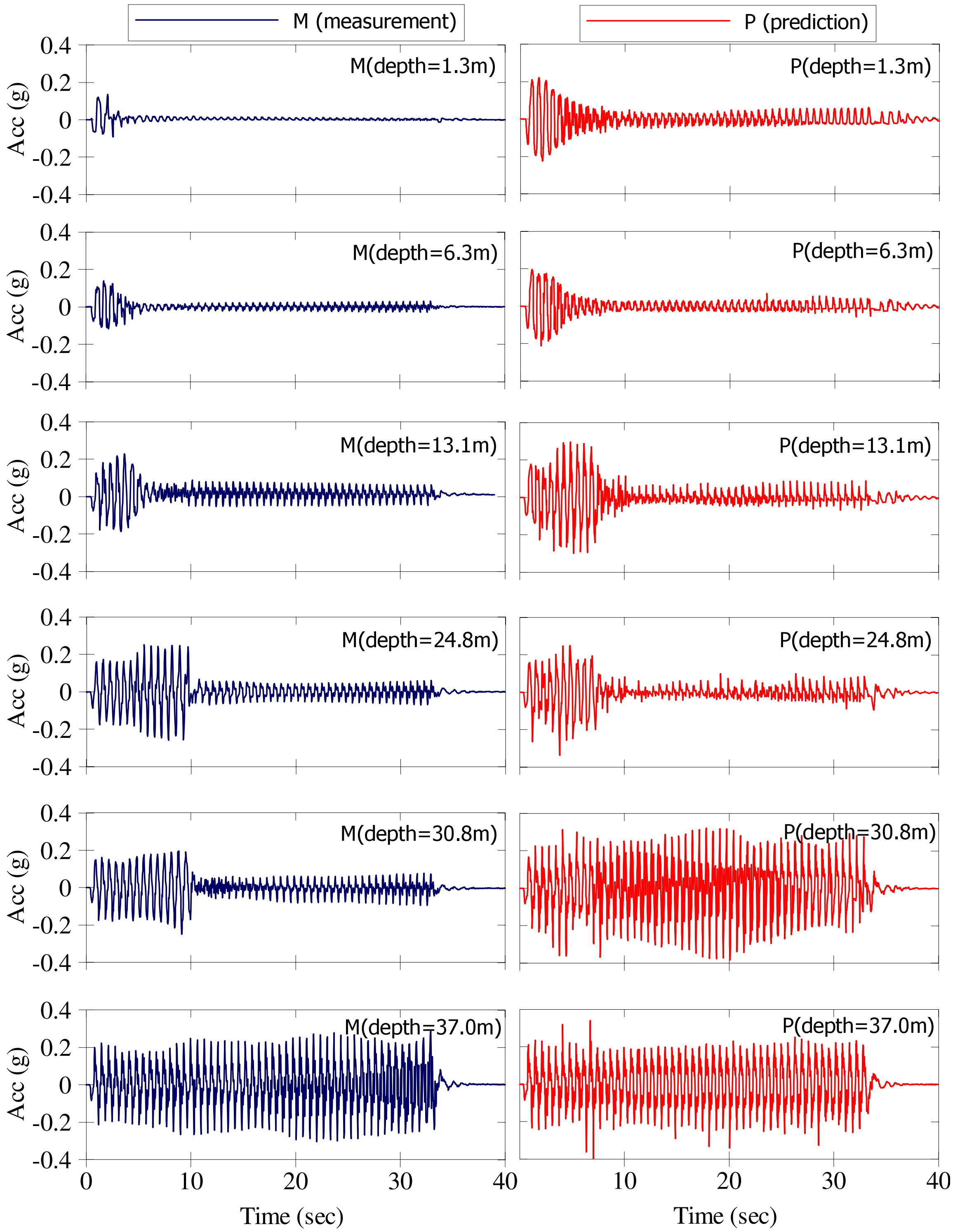

Fig. 9(a) Comparison between measured and predicted accelerations of Model 1

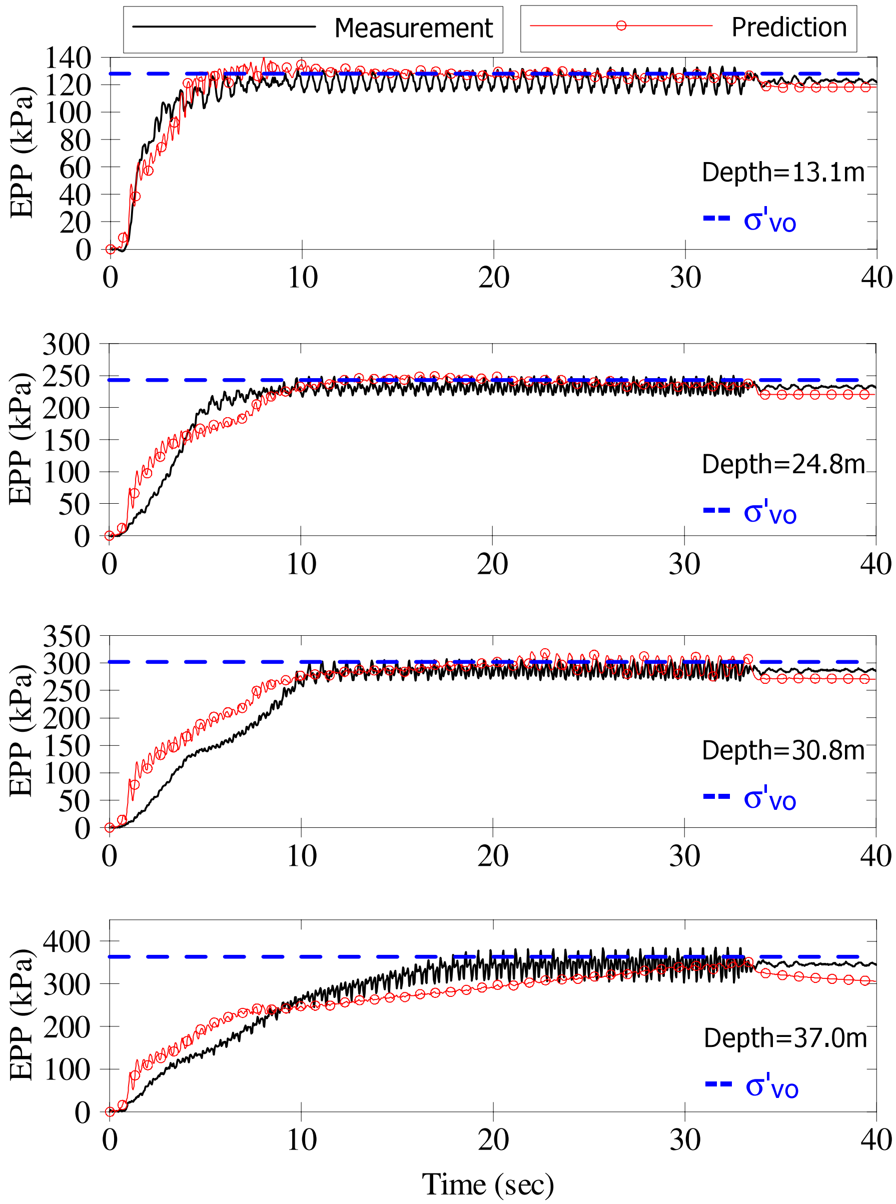

Fig. 9(b) Comparison between measured and predicted excess pore pressures of Model 1

Results for RPI Model 2

A cross-section of Model 2, showing the locations of the pore pressure transducers and accelerometers together with the FLAC simulation model, is shown in Fig. 10. In this model the lower portion was placed at D_r = 55 % and the upper at D_r = 75 % and a surface load was applied. The applied base motion is shown in Fig. 11. The effect of stress densification on relative density, D_r is shown in Fig. 12 and indicates that D_r has increased from 75 % to 81 % in the dense layer, and from 55 % to 63 % in the bottom loose layer.

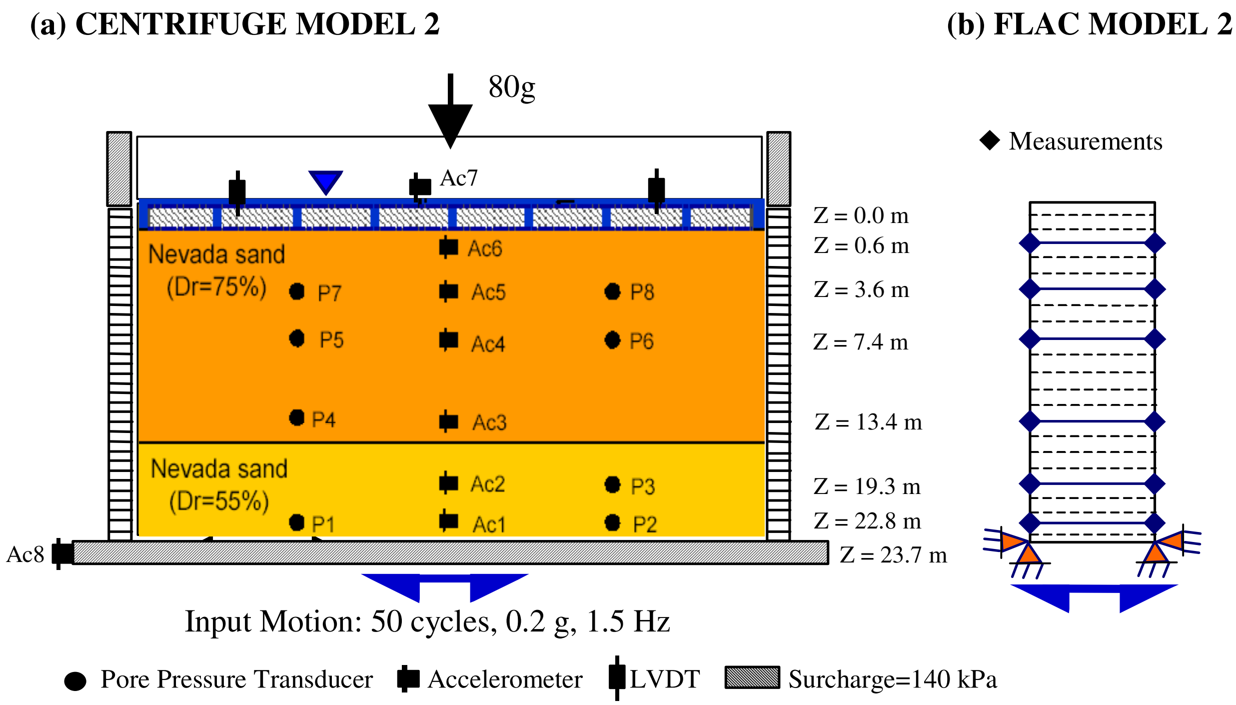

Fig. 10 Centrifuge Model 2 setups and FLAC Model 2 measurements

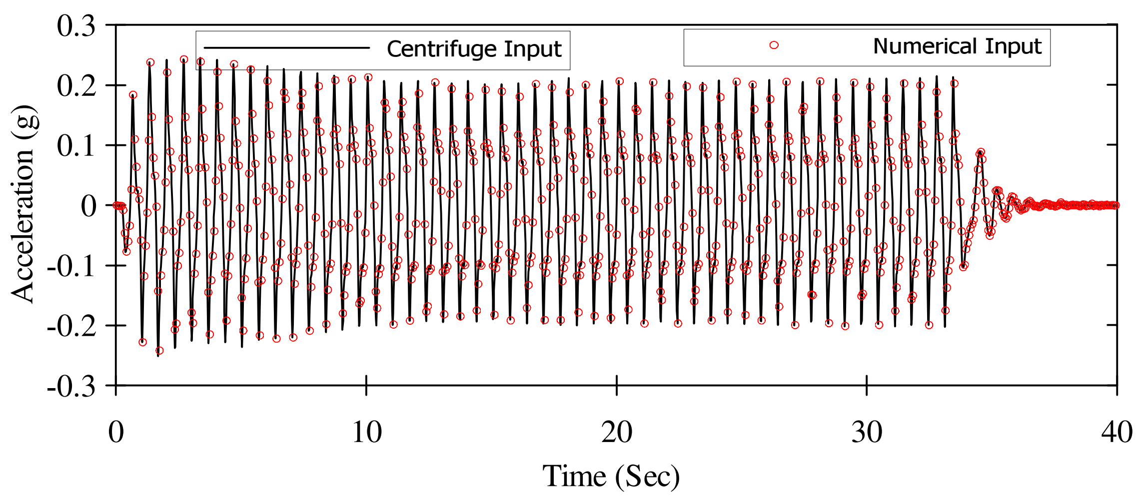

Fig. 11 Base input motions of Model 2

The predicted and measured accelerations and excess porewater pressures at prototype depths ranging from 0.6 m to 22.8 m are shown in Figs. 13a and 13b. It may be seen that, apart from the depth of 13.4 m, the predicted and measured acceleration responses are in general agreement. However, the predicted initial accelerations are significantly higher than the measured values in the first few seconds at shallower depths.

The predicted and measured excess pore pressures are also in reasonably good agreement except for the depth of 19.3 m where the predicted response is too rapid compared to the measured values. It may be seen that the denser upper layers, while they generate significant porewater pressure, do not liquefy.

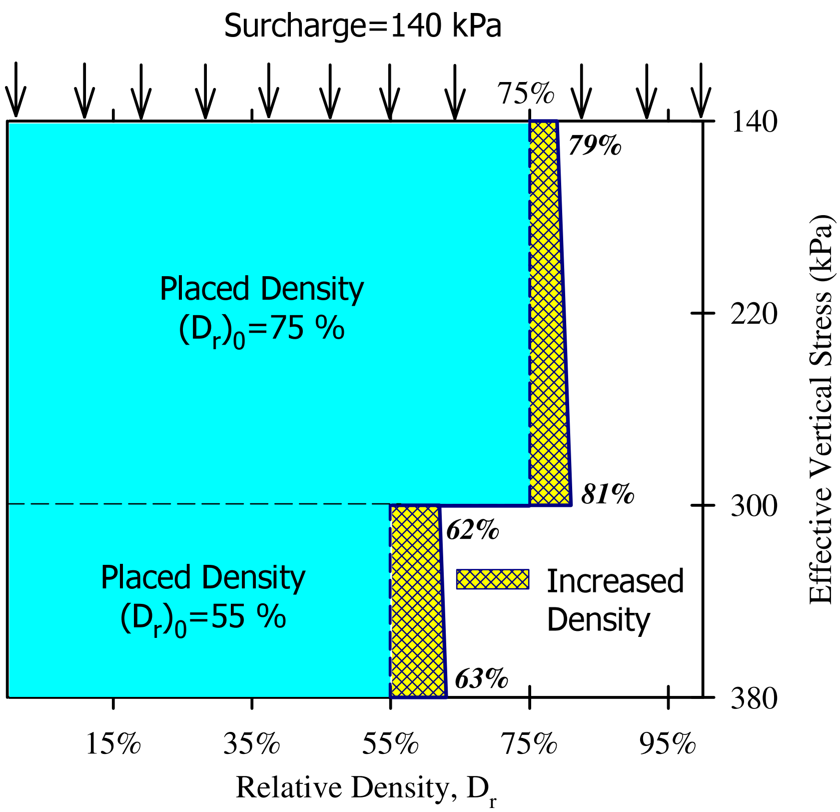

Fig. 12 Placed density and increased density of Model 2

The predicted accelerations in Fig. 13a indicate decoupling is occurring at about 4 sec at depths above 13.4 m. The predicted pore pressures in Fig. 13b indicate high pore pressures occurred at depth 19.3 m after about 4 sec, with R_u = 70%. This is not enough to base isolate and cause decoupling. So why the decoupling at 4 sec? The looser sand begins at depth 15 m and it is likely that liquefaction would first occur at or close to this depth. An examination of predicted response at depths in addition to the observed points shows that liquefaction, with R_u = 100 %, first occurred at a depth of 15 m at a time of 4 sec, and this explains the predicted response.

The measured response of Model 2 is more difficult to explain. The measured pore pressures in Fig. 13b show a 100 % pore pressure rise at depth 19.3 m after 20 sec. This should have caused decoupling of accelerations at all depths above 19.3 m after 20 sec. Instead the measured accelerations indicate a gradual decoupling occurring above a depth 7.4 m during the time period 0 to 20 sec. The abrupt reduction in rate of pore pressure generation at depth 19.3 m, Fig. 13b, after about 3 sec indicates an abrupt reduction in cyclic stress ratio occurred at this time. This could have been brought about by liquefaction occurring near the top of the loose layer at a time of about 3 sec, in agreement with expected and predicted response.

Both the measured and predicted pore pressures show that liquefaction did not occur in the denser sand above a depth of 7.4 m. Liquefaction did occur in the denser sand at depth 13.4 m after 30 sec due to upward drainage from the looser layer below 15 m. Liquefaction also occurred in the looser sand below a depth of 15 m at the 2 measurement locations after about 20 sec.

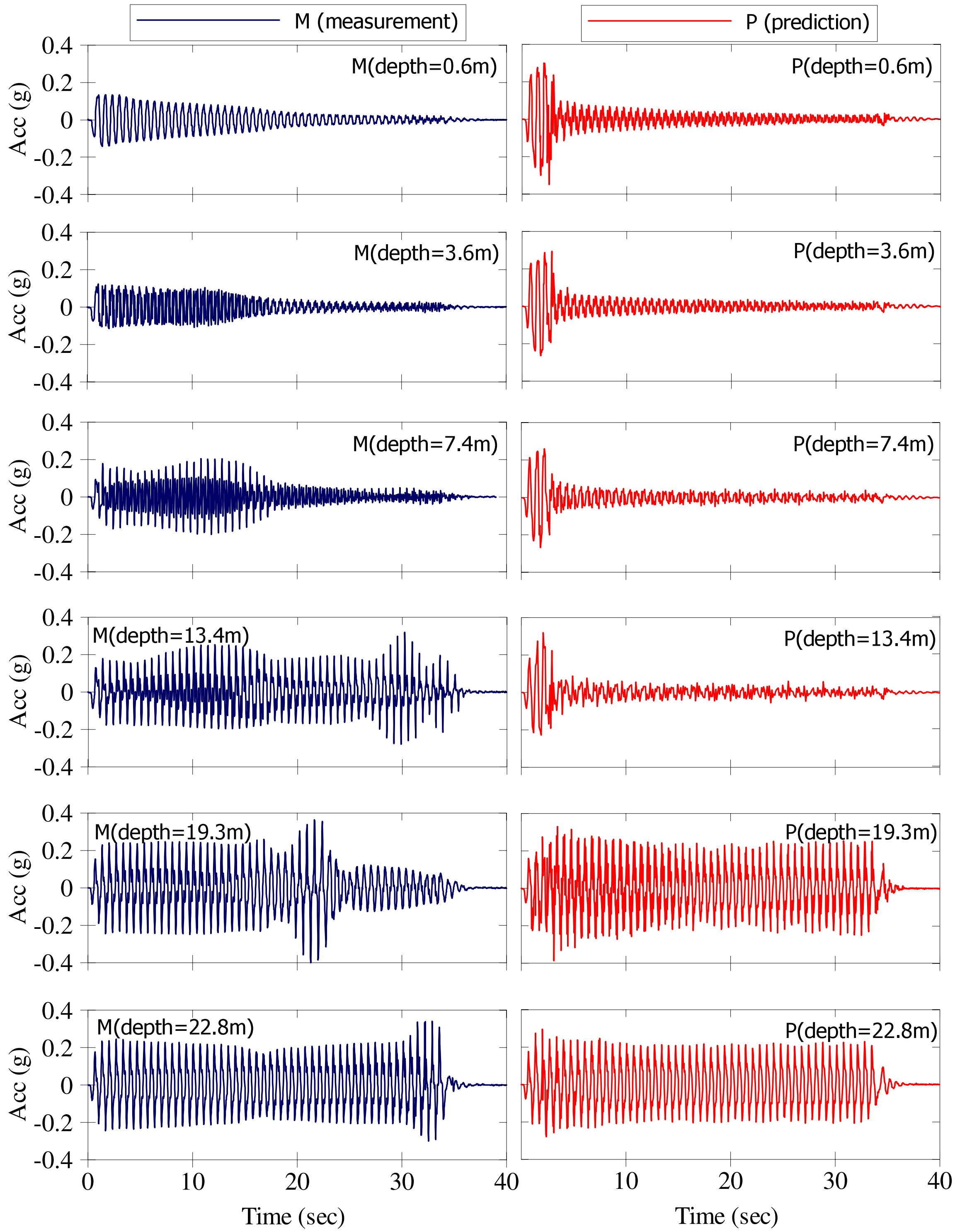

Fig. 13(a) Comparison between measured and predicted accelerations of Model 2

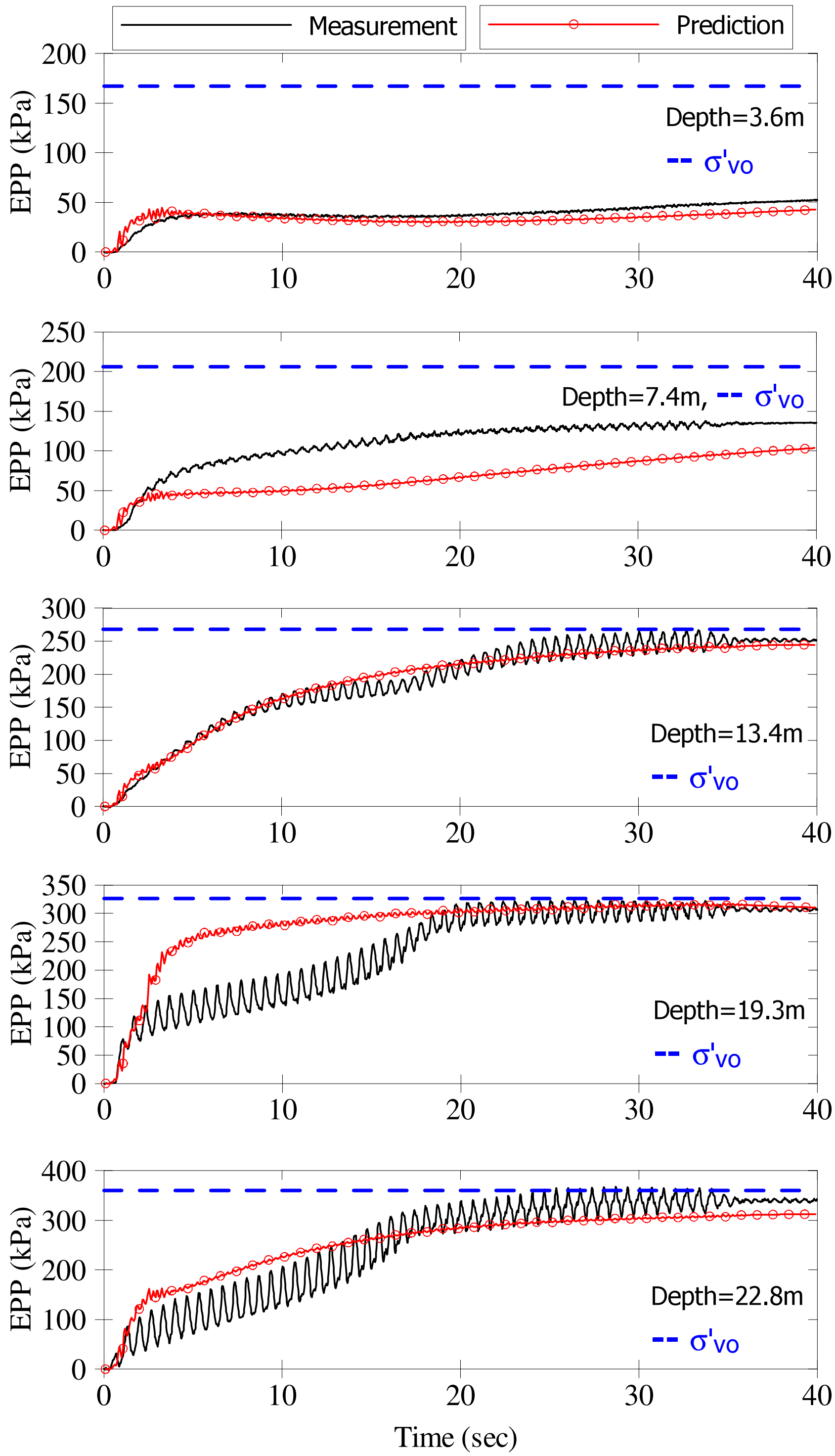

Fig. 13(b) Comparison between measured and predicted excess pore pressures of Model 2

Pore pressure spikes are much more noticeable in Model 2 that include a surcharge load and may arise from induced rocking which was not modeled in the numerical analysis.

Results for ERDC Model 5a

A cross-section of Model 5a, showing the locations of the pore pressure transducers and accelerometers together with the FLAC simulation model is shown in Fig. 14. In this model the lower portion was placed at D_r = 51 % and the upper at D_r = 72 % and a surface load of 580 kPa was applied. The applied base motion is shown in Fig. 15. Results from the FLAC simulation are shown for an initial saturation of 98% with densification.

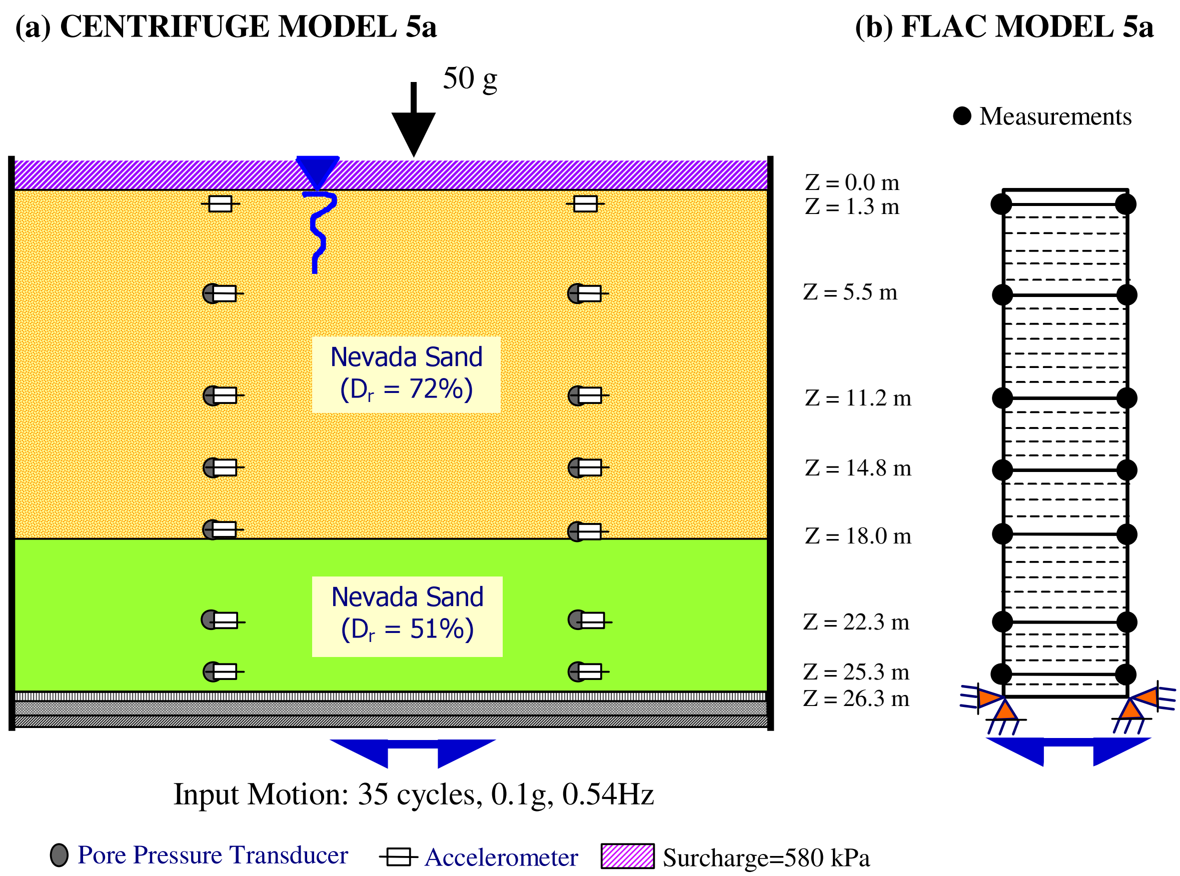

Fig. 14 Centrifuge Model 5a setups and FLAC Model 5a measurements

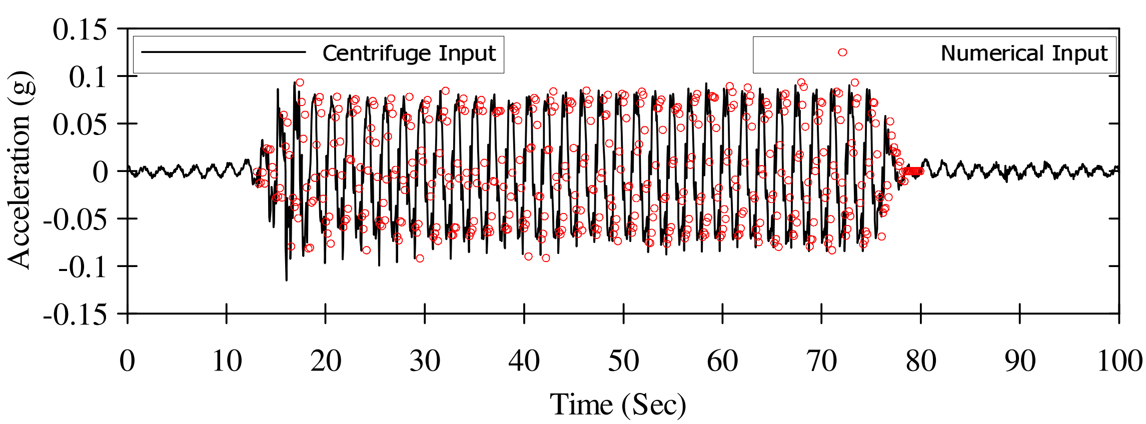

Fig. 15 Base input motions of Model 5a

The predicted and measured accelerations and excess porewater pressures at prototype depths ranging from 5.5 m to 25.3 m are shown in Figs. 16a and 16b. It may be seen that the predicted pore pressures are in good agreement except 25.3 m and the predicted accelerations higher than measured for an initial saturation, S_{r0} = 98 % with densification. Without stress densification liquefaction was predicted at 25.3 m.

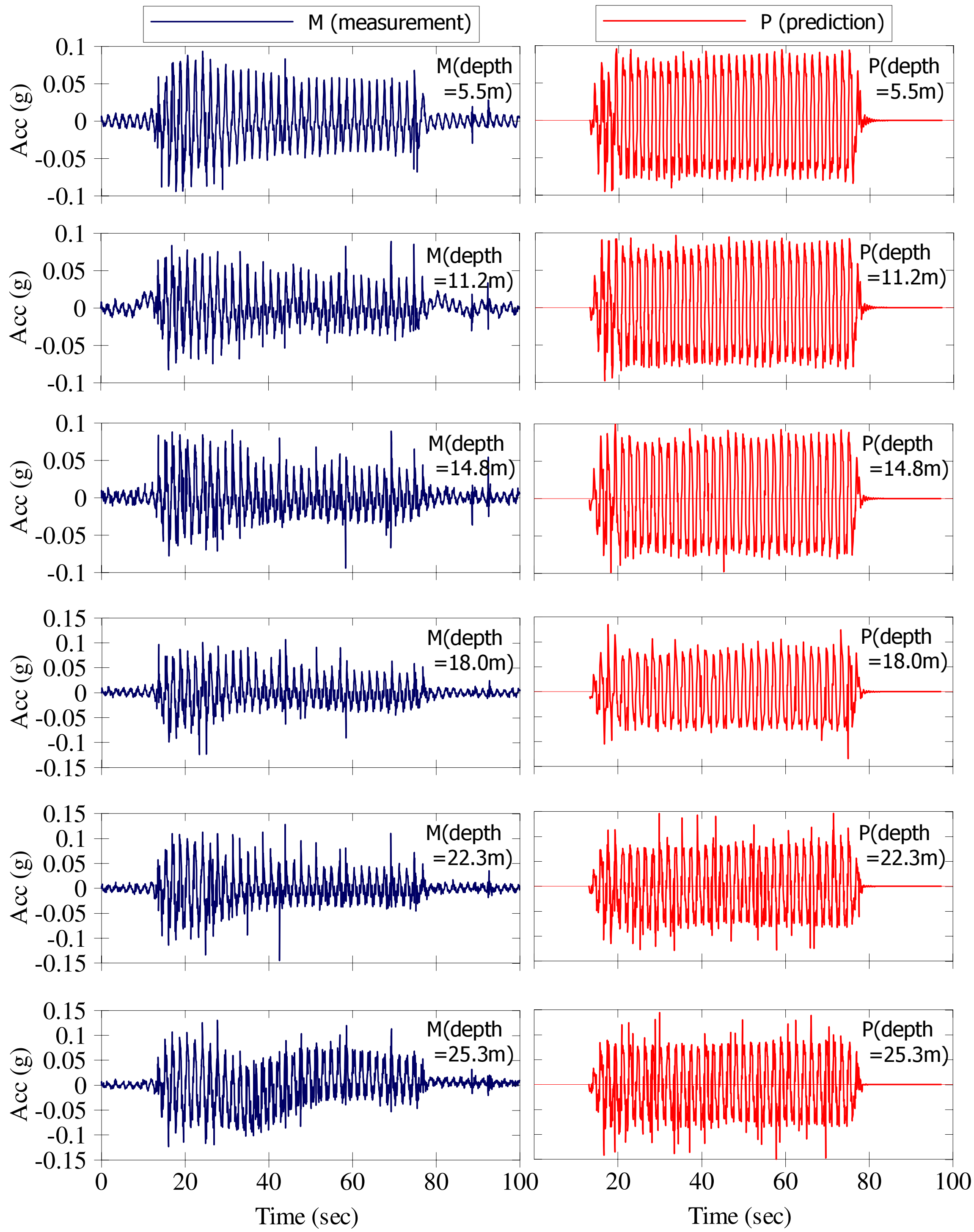

Fig. 16(a) Comparison between measured and predicted accelerations of Model 5a, S_{r0}=98 % with densification

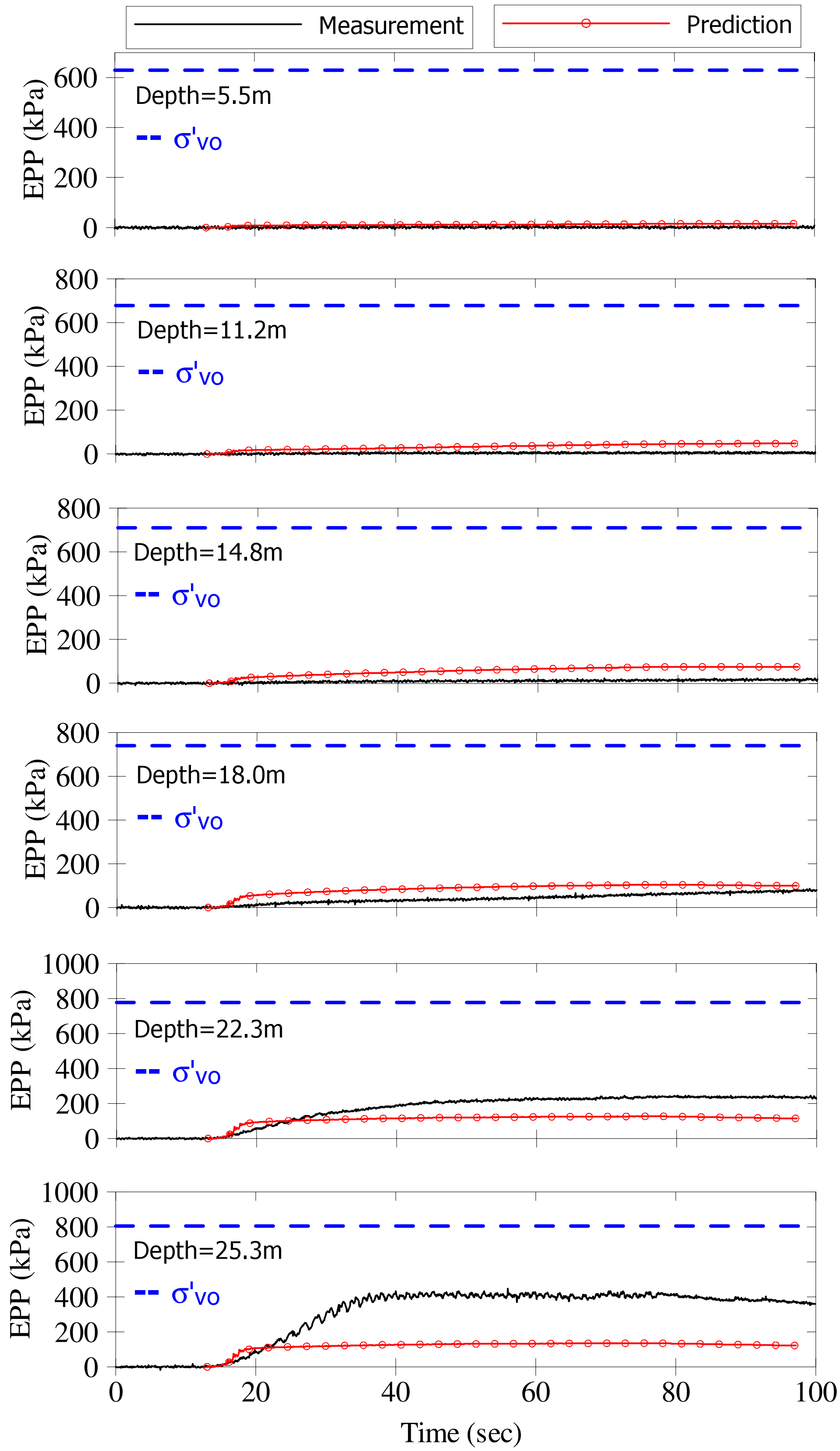

Fig. 16(b) Comparison between measured and predicted excess pore pressures of Model 5a, S_{r0}=98 % with densification

SUMMARY

Conventional liquefaction assessment procedures indicate that liquefaction can occur to considerable depths in loose to medium dense sand strata. This is based on dynamic analysis and the results of element tests showing that liquefaction resistance ratio reduces with increased confining stress, the K_σ effect. Pore pressure measurements in better-saturated centrifuge models conducted at RPI indicate that liquefaction occurred at considerable depths (corresponding to an overburden stress of 300 kPa or more) in loose or medium dense sand strata. In centrifuge models where liquefaction occurred at large depths, the models did show trends in the development of pore pressure and liquefaction that were not consistent with state of practice or with state-of-art liquefaction analysis. Numerical analyses were performed that indicate the centrifuge findings can be explained in terms of the densification that occurs when high confining stresses are imposed. Thus a sand that was placed at D_r = 55 % densifies to D_r = 63 % at an applied confining stress of 380 kPa. This change in density can explain the development of liquefaction at the ground surface first with later propagation downward through the rest of the model.

Some ERDC centrifuge tests simulating the response of a level ground sand system to seismic loading indicated that liquefaction was curtailed at high confining stress in the 300 kPa region. Thus the results of these centrifuge tests appeared to be in conflict with both standard procedure and RPI centrifuge tests. Numerical analyses indicate that these centrifuge findings can be explained in terms of stress densification and lack of saturation.

Stress densification will also occur under field conditions and will improve liquefaction resistance. However, it is accounted for in principle in conventional liquefaction assessment techniques that are based on penetration resistance by correcting for confining stress. Penetration resistance value so corrected are a measure of relative density and so should reflect density changes arising from stress densification as well as other factors such as changes in depositional environment.

REFERENCES

1. Youd T.L., Idriss I.M., Andrus R.D., Arango I., Castro G., Christian J.T., Dobry R., Finn W.D.L., Harder Jr. L.F., Hynes M.E., Ishihara K., Koester J.P., Liao S.S.C., Marcuson III W.F., Martin G.R., Mitchell J.K., Moriwaki Y., Power M.S., Robertson R.K., Seed H.B., and Stokoe II K.H. "Liquefaction resistance of soils: summary report from the 1996 NCEER and 1998 NCEER/NSF workshops on evaluation of liquefaction resistance of soils." Journal of Geotechnical and Geoenvironmental Engineering, 2001; 127(10): 817-833.
2. Steedman R.S., Ledbetter R.H. and Hynes M.E. "The influence of high confining stress on the cyclic behavior of saturated sand." Soil dynamics and liquefaction 2000: *In* Proceedings of the Sessions of Geo-Denver 2000: August 5-8, 2000, Denver, Colorado, 35-57.
3. Arulanandan K. and Scott R.F. "Verification of numerical procedures for the analysis of soil liquefaction problems." *In* Proceedings of the International Conference on the Verification of Numerical Procedures for the Analysis of Soil Liquefaction Problems, 1993, Vols. 1 and 2, Balkema, Rotterdam, the Netherlands.
4. Dafalias Y.F. "Bounding surface plasticity. I: mathematical foundation and the concept of hypoplasticity." Journal of Engineering Mechanics, 1986; 112(9): 966-987.
5. Prevost J.H. "DYNA1D: A computer program for nonlinear site response analysis." Technical Report No. NCEER-89-0025, 1989, National Center for Earthquake Engineering Research, SUNY at Buffalo, NY.
6. Zienkiewicz O.C., Chan A.H.C., Pastor M., Paul D.K. and Shiomi T. "Static and dynamic behavior of soils: a rational approach to quantitative solutions. Part I: fully saturated problems." *In* Proceedings of the Royal Society of London, Mathematical and Physical Sciences, 1990, Series A, 429: 285-309.

7. Byrne P.M., Roy D., Campanella R.G. and Hughes J. “Predicting liquefaction response of granular soils from pressuremeter tests.” ASCE National Convention, San Diego, Oct. 23-27, 1995, ASCE, Geotechnical Special Publication 56: 122-135.
8. Beaty M. and Byrne P.M. “An effective stress model for predicting liquefaction behaviour of sand.” Geotechnical Earthquake Engineering and Soil Dynamics III. *Edited by* P. Dakoulas, M. Yegian, and R Holtz (eds.), 1998, ASCE, Geotechnical Special Publication 75 (1): 766-777.
9. Elgamal A.-W., Parra E., Yang Z, Dobry R. and Zeghal M. “Liquefaction constitutive model.” *In* Proceedings of the International Workshop on the Physics and Mechanics of Soil Liquefaction. Baltimore, Maryland, USA, 1999; pp. 269-279.
10. Kramer S., and Arduino P. “Constitutive modeling of cyclic mobility and implications for site response.” *In* Proceedings of the Second International Conference on Earthquake Geotechnical Engineering, Balkema, Rotterdam, The Netherlands. 1999, Vol. 3, pp. 1029-1034.
11. Puebla H., Byrne P.M. and Phillips R. “Analysis of CANLEX liquefaction embankments: prototype and centrifuge models.” Canadian Geotechnical Journal, 1997, 34: 641-657.
12. Byrne P. M., Park S.-S., Beaty M., Sharp M., Gonzalez, L. and Abdoun, T. “Numerical modeling of liquefaction and comparison with centrifuge tests.” Canadian Geotechnical Journal, 2004, 41(2) (in press).
13. Hardin B.O. “The nature of stress-strain behavior for soils.” *In* Proceedings of the ASCE Geotechnical Engineering Division Specialty Conference on Earthquake Engineering and Soil Dynamics, 1978, 1: 3-90.
14. Itasca. FLAC, version 4.0. 2000, Itasca Consulting Group Inc., Minneapolis.
15. Gonzalez L., Abdoun T. and Sharp M.K. 2002. “Modelling of seismically induced liquefaction under high confining stress.” International Journal of Physical Modelling in Geotechnics, 2002, 2(3): 1-15.
16. Park S.-S. and Byrne P.M. “Stress densification and its evaluation.” Canadian Geotechnical Journal, 2004, 41(1): 181-186.
17. Arulmoli K., Muraleetharan K.K., Hosain M.M. and Fruth L S. “VELACS laboratory testing program, soil data report.” The Earth Technology Corporation, Irvine, California, Report to the National Science Foundation, Washington D.C., March, 1992.
18. Kammerer A., Wu J., Pestana J., Riemer M. and Seed R. “Cyclic simple shear testing of Nevada sand for PEER Center project 2051999.” Geotechnical Engineering Research Report No. UCB/GT/00-01, University of California, Berkeley, January 2000.